

PATRYCJA WASZCZUK-ZELLNER¹, MARCIN LUTYŃSKI²,
ALEKSANDRA KOTERAS^{3*}

FACTORS INFLUENCING POTENTIAL CO₂ STORAGE CAPACITY IN SHALES

This article aims at presenting research on the sorption of carbon dioxide on shales, which will allow to estimate the possibility of CO₂ injection into gas shales. It has been established that the adsorption of carbon dioxide for a given sample of sorbent is always greater than that of methane. Moreover, carbon dioxide is the preferred gas if adsorption takes place in the presence of both gases. In this study CO₂ sorption experiments were performed on high pressure setup and experimental data were fitted into the Ambrose four components models in order to calculate the total gas capacity of shales as potential CO₂ reservoirs. Other data necessary for the calculation have been identified: total organic content, porosity, temperature and moisture content. It was noticed that clay minerals also have an impact on the sorption capacity as the sample with lowest TOC has the highest total clay mineral content and its sorption capacity slightly exceeds the one with higher TOC and lower clay content. There is a positive relationship between the total content of organic matter and the stored volume, and the porosity of the material and the stored volume.

Keywords: CO₂ storage; storage capacity; storage in shales; CO₂ sorption

1. Introduction

Due to extraction of crude oil and natural gas, traditional deposits of these two natural resources are continuously shrinking. The solution for reduced supply of energy obtained from listed sources is extracting natural gas from shales. Shale gas (also called as tight gas, although they are not the same) became more popular source of natural gas in USA since its first commercial use

¹ LNPC PATRYCJA WASZCZUK, PSZCZYNA, POLAND

² SILESIAN UNIVERSITY OF TECHNOLOGY, 2A AKADEMICKA STR., 44-100 GLIWICE, POLAND

³ CENTRAL MINING INSTITUTE (GIG), 1 GWARKÓW SQ., 40-166 KATOWICE, POLAND

* Corresponding author: akoteras@gig.eu



© 2022. The Author(s). This is an open-access article distributed under the terms of the Creative Commons Attribution-NonCommercial License (CC BY-NC 4.0, <https://creativecommons.org/licenses/by-nc/4.0/deed.en>) which permits the use, redistribution of the material in any medium or format, transforming and building upon the material, provided that the article is properly cited, the use is noncommercial, and no modifications or adaptations are made.

in early '80 in Barnett, Texas [1]. In the last decade revolution in American fuel's politic became fact, when USA transformed from importer of shale gas to its exporter and a half of a natural gas extracted on USA territory is obtained from shales, what makes it the biggest shareholder of shale gas market [2,3].

Shale gas deposits are very common all over the world and have a similar structure – they consist of organic matter and clay minerals, with almost negligible permeability. This poses huge mining problems starting with the necessity of deep wells drilling and fracturing. Fractures allow the gas to flow yet there is a difficulty of maintaining the light of the obtained fractures and for that purpose proppants are used. In comparison to conventional gas wells, shale gas wells produce at lower rates however the advantage is the longer production time up to tens of years from a single well [4]. There are also ideas to enhance shale gas recovery by CO₂ injection. In this approach carbon capture and storage mixed with extracting gas has a positive energy balance [5,6]. This allows not only to obtain more shale gas but also helps in reducing the footprint left by gas production [7].

This article aims at presenting research on the sorption of carbon dioxide on shales, which will allow to estimate the possibility of CO₂ injection into the volume of shale rocks. The clay minerals such as kaolinite, illite, montmorillonite and chlorite in the shale rocks are known for their good sorption properties. This allows to assume common statement that sorption occurs mostly on organic content of shale since part of the gas is sorbed in clay minerals, this can lead to underestimation of amount of carbon dioxide which can be stored in shale reservoir.

In previous studies it has been established that the adsorption of carbon dioxide for a given sample of the material is always greater than that of methane [8]. Moreover, carbon dioxide is the preferred gas if adsorption takes place in the presence of both gases [9]. It is known that the greater the content of organic matter in shale, the greater its suitability as a source of shale gas and a carbon dioxide reservoir [10,11]. Also, the common knowledge is that presence of clay minerals has a positive effect on the sorption capacity of shale, but this is usually marginal in case of high content of organic matter [12,13]. When organic content is particularly low and does not exceed 1% of mineral composition, then sorption occurs on clay minerals almost exclusively, although amounts of sorbed gas are significantly lower than with higher organic content [14,15].

The shale storage capacity for carbon dioxide allows to calculate the amount of gas, which can be injected into shale formation and trapped in pores and voids as well as with bonding surface mechanism in porous solid. The mechanism is not homogenous and can be considered as adsorption on rock surface, dissolution and other (in much lesser extent) phenomena [16]. As shales present nearly negligible permeability appearing together with seal over the petroleum reservoirs they are considered as attractive place for carbon dioxide sequestration. Another advantage is preference in sorption CO₂ over the natural gas due to molecular swapping mechanism, which is promoting methane to desorb and staying in free phase while CO₂ is sorbed on pores surface.

2. Materials and methods

For the purpose of research, shale rocks with low total organic content (TOC) and high mineral content were chosen. Silurian-Ordovician shale rocks were sampled from the northern part of the Baltic – Podlasie – Lublin basin (Fig. 1). Due to the non-disclosure agreement the exact location of exploratory well and sample depths cannot be revealed. Shale rocks are divided into samples obtained from different depths which significantly differ in amount of clay

minerals and TOC content. Two pair of samples were chosen for tests, 2 with higher and 2 with lower TOC content, in order to show variation in gas storage capacity. Mineral composition of samples was measured using X-ray diffraction (XRD) and the TOC content using rock-eval method (see Table 1).



Fig. 1. Location of Baltic-Podlasie-Lublin basin. Samples were collected from the northern part. Due to non-disclosure agreement the exact location cannot be revealed [17]

TABLE 1

Samples composition based on XRD and rock-eval test (TOC)

No.	Carbonate minerals wt. %	TOC wt. %	Kaolinite wt. %	Montmorillonite + illite wt. %	Chlorite wt. %	Clay minerals total wt. %
1	11,6	0,98	0,7	44,6	7,4	52,7
2	2,5	0,3	1	58,5	3	62,5
3	3,5	6,66	0	50,7	7,1	58,9
4	2,1	7,22	0,9	51,8	4,5	57,2

The sorption tests were conducted with in-house designed and made manometric apparatus (Fig. 2). The set consists of gas cylinder, compressor, high-performance pump Maximator DLE

5-30-GG, vacuum pump and thermostatic bath with temperature adjustment with an accuracy of $0,1^{\circ}\text{C}$. Internal part of a setup is immersed in thermostatic bath and consists of double set of reference (RC) and sample (SC) cells which allows conducting two tests at once. The elements are linked with ball valves and Swagelok high-pressure stainless-steel fittings. Apparatus is connected to data collecting system. Set of pressure sensors Keller Druck X33 (0.05% FS 0-200 bar) with a measurement accuracy of up to 0.02 bar and 0.01K are located inside the cells and temperature sensors PT-100 class 1 / 10B located inside the reference cells and sample cells. Temperature data are recorded in data logger L200-RTD.

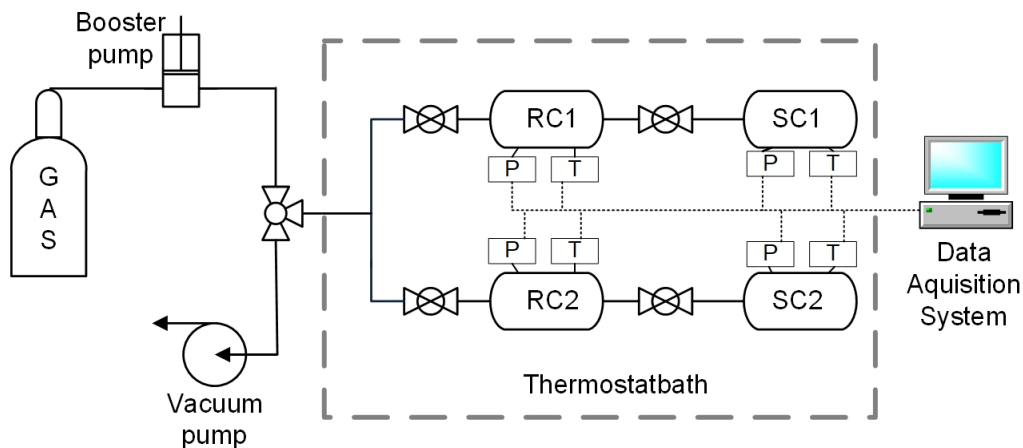


Fig. 2. High pressure manometric setup for sorption measurement

Samples were ground below 0.1 mm and dried in accordance with the PN-80 / G-04511 norm, cooled in desiccator to avoid moisture saturation and then inserted into sample cell. The apparatus was sealed, closed, and calibrated with helium. Helium as inert gas does not take part in sorption and this property allows to determine the volume of reference cells and the free volume of the sample cell. Helium remained in the apparatus for 24 hours to check the tightness and increase the possible gas penetration into the sample. Then inert gas was vacuumed to degas the samples from possible residues of adsorbed gases.

This step preceded main sorption test, which was conducted iteratively and included repetitive steps:

1. gas injection and temperature stabilization – the valve between RC and SC is closed; time: approx. 1 h
2. connecting gas and sample, the valve is opened;
3. sorption observation, collecting temperature and pressure value every 5 sec, time: approx. 24 h;
4. closing valve between samples, start of injecting next portion of gas into RC as in step 1.

The manometric method of sorption testing is measuring the pressure reduction in the system, caused by the transition of gas molecules from the free phase to the subsurface adsorbed phase. It is assumed that under constant conditions (here: temperature and volume) the pressure reduc-

tion in the system is directly proportional to the amount of sorbed gas, hence sorbed gas can be calculated as subtraction of total injected gas and gas staying in not-sorbed state:

$$n_{sorbed} = n_{total} - n_{free} \quad (1)$$

Here n_{sorbed} is number of moles of adsorbed gas, n_{total} is the total number of moles of gas in the system, and n_{free} is the number of moles of free gas, all values in mmol.

The number of moles of free gas is the product of the volume available for the injected gas (void volume of the apparatus and volume of pores penetrated by gas) and the density of the gas at a constant temperature and pressure:

$$n_{free} = V_m \cdot \rho^{p,T} \quad (2)$$

The density of Helium was calculated with a McCarthy equation of state [18]. The density of carbon dioxide was calculated with the Span&Wagner equation of state [19] and CH₄ was calculated with Wagner&Setzmann [20].

The mass of gas, transferred in one step can be calculated with below equation:

$$n_z = \sum_{i=1}^n Y_{ref} \cdot (\rho_i^f - \rho_i^e) \quad (3)$$

where ρ_i^f is the gas density before injection additional portion of gas and after stabilization of the temperature in whole volume of apparatus? This equation is necessary to establish a sorption isotherm.

3. Results

3.1. Sorption isotherms

Experimental data points were fitted with two parameter Langmuir model for absolute adsorption:

$$a_{abs} = \frac{a_m \cdot \rho_g}{b_v + \rho_g} \quad (4)$$

and three parameter Langmuir model for excess adsorption:

$$a_{exc} = \frac{a_m \cdot \rho_g}{b_v + \rho_g} \left(1 - \frac{\rho_g}{\rho_s} \right) \quad (5)$$

Here a_{exc} the excess sorption, a_m is the maximum monolayer capacity, b_v is the Langmuir equilibrium constant, equal $1/P_L$, ρ_g is the free phase gas density and ρ_s is the adsorbed phase gas density. Calculation of Langmuir parameters and fitting the model to experimental data was achieved with minimizing residual sum of squares to the experimental data with EXCEL solver. Four experimental measurements were conducted at the temperature of 50°C and 80°C, in pressure range 0 to 10 MPa. Results of tests for all the samples are presented in Figures 3, 4, 5 and 6 as the sorbed volume (in mmol/g) against pressure below.

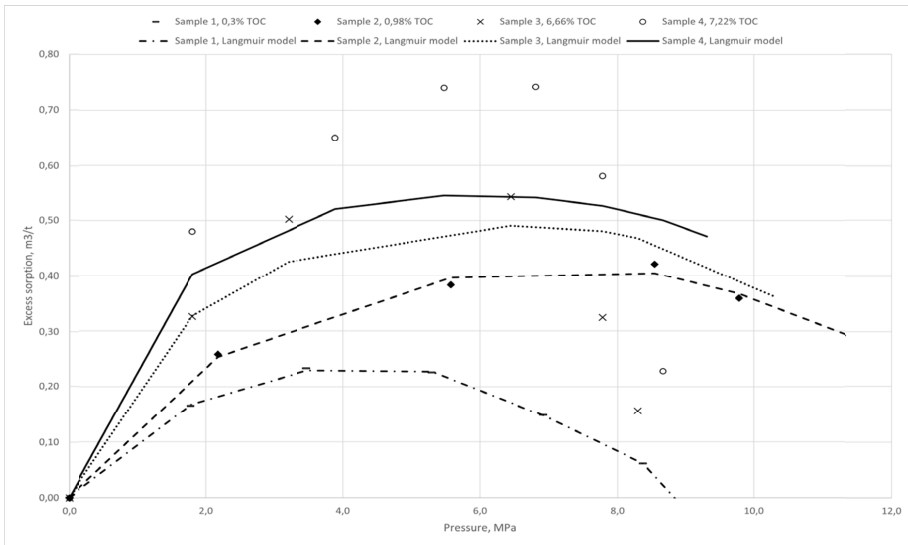


Fig. 3. Carbon dioxide excess sorption isotherms on samples at 50°C

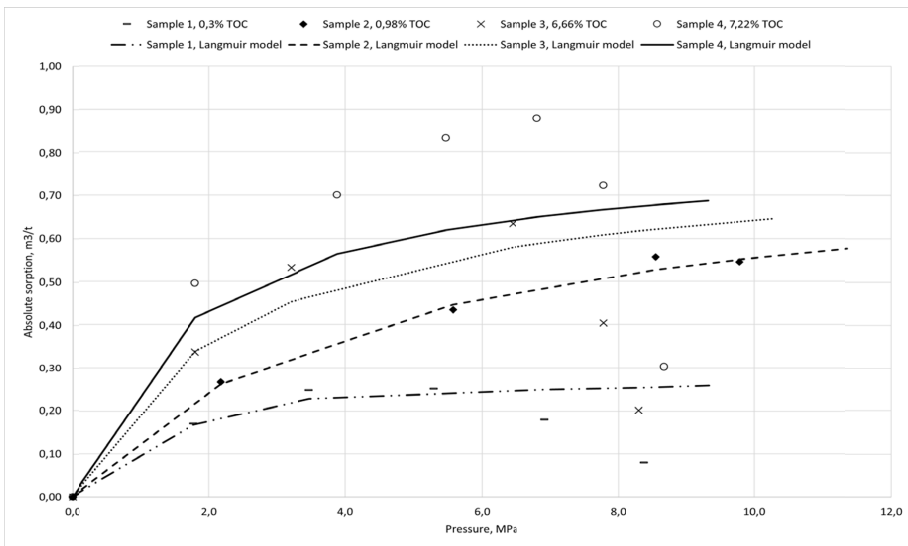


Fig. 4. Carbon dioxide absolute sorption isotherms on samples at 50°C

Adsorption isotherms (Fig. 3 to Fig. 6) show that total organic content is correlated with higher sorption capacity. Figure 7 presents Langmuir volume plotted against the TOC which shows that sorption is almost directly proportional to organic content.

A significant drop of isotherm can be observed when pressure in setup reaches 8 MPa at 50°C and 6 MPa at 80°C. This phenomena can be explained by various factors i.e.: low adsorbed phase

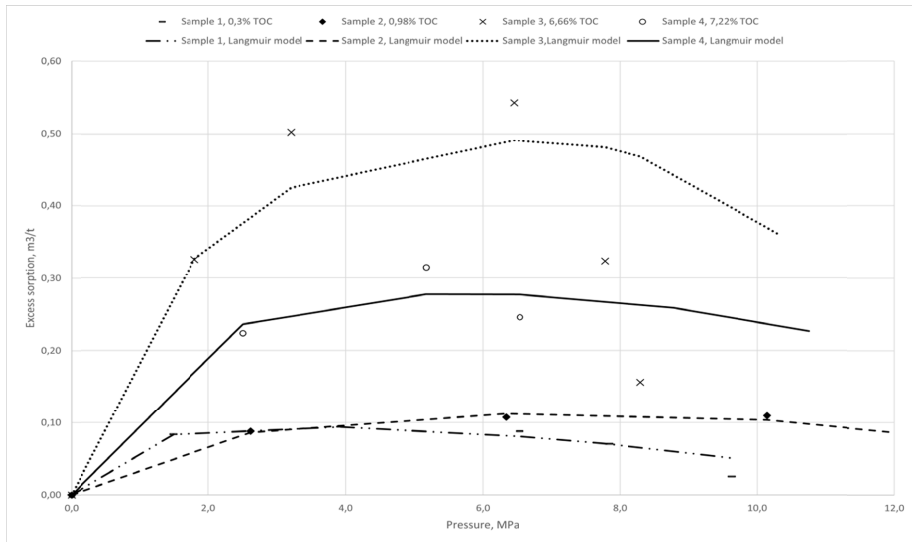


Fig. 5. Carbon dioxide excess sorption isotherms on samples at 80°C

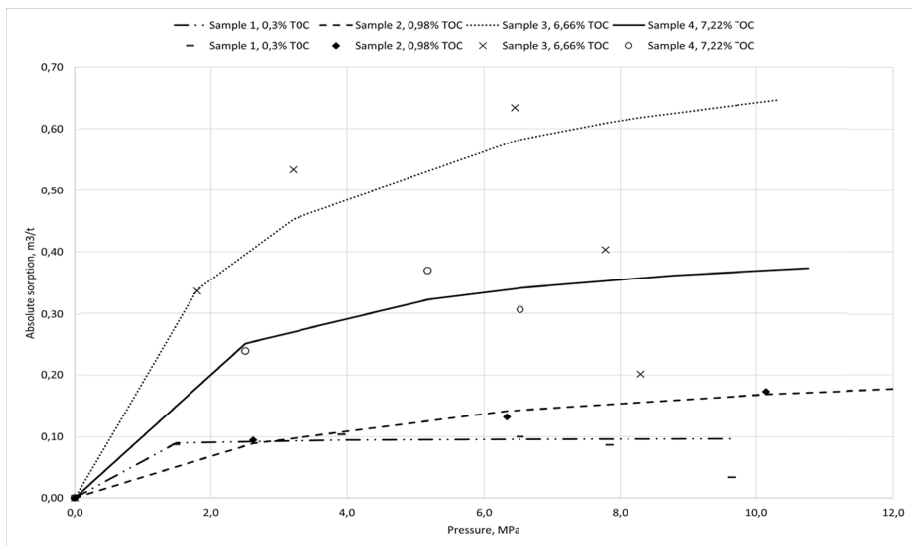


Fig. 6. Carbon dioxide absolute sorption isotherms on samples at 80°C

density (sorption energy) of dry shales and experimental artifacts behavior of CO_2 near critical point. Further explanation of this phenomena can be found in [6,21]. The fitting of Langmuir model is considerably good up to the pressure of 6-8 MPa where the experimental points drop. Discrepancy between the experimental points and model can be attributed to the phenomena mentioned above where the mismatch increases with pressure. Results of experiments also

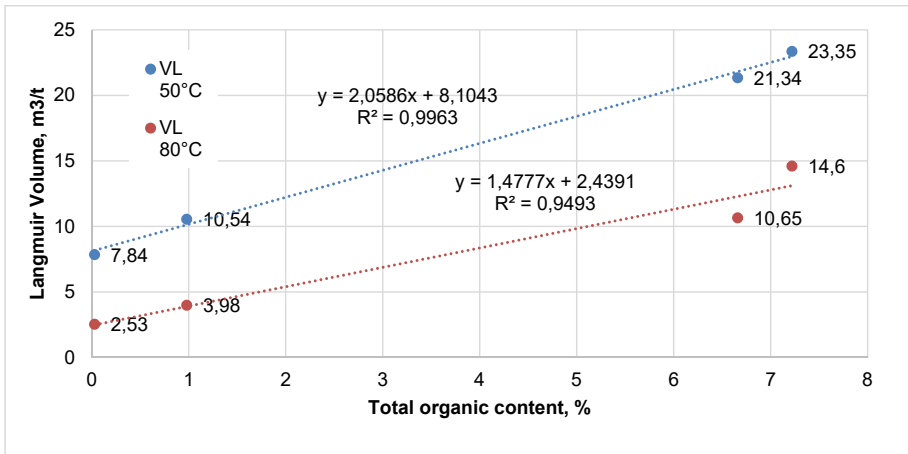


Fig. 7. The relationship between the Langmuir volume and total organic content

show that sorption capacity is inversely proportional with the temperature. In Table 2 Langmuir parameters calculated using the equation (5) for isotherms are presented.

TABLE 2

Langmuir parameters calculated for the samples

No	V_L CO ₂ , m ³ /t		P_L CO ₂ , MPa	
	50°C	80°C	50°C	80°C
1	7,84	2,53	5,83	1,13
2	10,54	3,98	4,48	3,09
3	21,34	10,65	2,43	3,49
4	23,35	14,60	1,71	2,86

3.2. Storage capacity

Although there are several methods of estimating shale storage capacity [22-24] in this paper two methods proposed by Ambrose et al.: standard and with further modifications [25,26] have been used for comparison.

The calculation is based on 4 components:

1. G_f , volumetric component, free gas storage capacity, representing on amount of gas stored in pores, based on modified standard reservoir evaluation methods.
2. G_a , surface component, adsorbed gas storage capacity, representing gas sorbed on surface area of pores, based on sorption isotherm measurements by establishing equilibrium adsorption isotherm.
3. G_{so} , second volumetric component, dissolved gas-in-oil storage capacity, representing gas solved in liquid hydrocarbons, component is combined with adsorbed gas capacity in reservoirs that contain a large fraction of liquid hydrocarbon in the pore space, has not been considered important.

4. G_{as} , third volumetric component, dissolved gas-in-water storage capacity, representing gas solved in formation water, estimated from the bulk solubility calculations, as above has not been considered important.

Hence basic calculation:

$$G_{st} = G_f + G_a + G_{so} + G_{sw} \quad (6)$$

As mentioned, G_{so} and G_{sw} has little to no importance therefore are not applicable:

$$G_{st} = G_f + G_a \quad (7)$$

G_f according to the standard method:

$$G_f = 32,0368 \frac{\varphi(1-S_w)}{\rho_b B_g} \quad (8)$$

Modification proposed in [3]:

$$G_f = \frac{32,0368}{B_g} \left[\frac{\varphi(1-S_w)}{\rho_b B_g} - \frac{1,318 \cdot 10^{-6} \dot{M}}{\rho_s} V_L \frac{P}{P+P_L} \right] \quad (9)$$

G_a stays unmodified in both versions:

$$G_a = V_L \frac{P}{P+P_L} \quad (10)$$

Here φ is total porosity fraction, S_w is saturation, B_g is gas formation volume factor, reservoir volume/surface volume, M is molecular weight of gas, V_L is Langmuir volume, P_L is Langmuir pressure, P is pressure, ρ_b – bulk rock density, ρ_s – sorbed phase density.

Total porosity, density and water saturation of samples are known. Molecular weight of gas and gas formation volume factor are constant. Langmuir volume and Langmuir pressure are obtained from previous volumetric method tests. The sorbed phase density is discussed and in literature different values are encountered [16]. Here 22 mmol/mol were taken as this value corresponds to the density of the gas in the liquid state. Two values of the porosity of the material were adopted for the calculations: 4.8% and 9.5%, which corresponds to the average and high porosity of gas-bearing shales [27]. The results are presented in Tables 3 and 4.

Data presented in tables 3 and 4 indicates that G_a component stays constant despite various moisture and porosity values as it is based on Langmuire volume and pressure, which were obtained from prepared samples. These two factors are not influencing the volume and pressure itself but rather time of sorption.

The G_f component is highly dependent on porosity and in both cases takes values twice higher. Also in Ambrose model this component is slightly higher than in classic one.

Figure 8 shows results for shale storage capacity for 4.8% porosity shale, 35% water saturation and 50°C reservoir temperature. Samples with lower TOC have amount of storage gas approx. 9 to 15 m³/t, while samples with higher TOC have amount of gas storage approx. 20 to 23 m³/t.

TABLE 3

Storage capacity for samples with moisture 30%. G values in m³/t

ϕ 4,8									
50°C					80°C				
Sample	TOC	G_a	G_f	G_{aAmbr}	G_{fAmbr}	G_a	G_f	G_{aAmbr}	G_{fAmbr}
1	0,3%	6,98	2,41	6,98	2,31	3,14	2,36	3,75	2,38
2	0,98%	9,94	2,36	9,94	2,25	2,00	2,41	2,26	2,41
3	6,66%	17,67	2,87	17,67	2,08	7,93	2,87	8,82	2,27
4	7,22%	20,67	2,15	20,67	2,02	9,93	2,15	12,92	2,19
ϕ 9,5									
50°C					80°C				
Sample	TOC	G_a	G_f	G_{aAmbr}	G_{fAmbr}	G_a	G_f	G_{aAmbr}	G_{fAmbr}
1	0,3%	6,98	4,15	6,98	4,72	2,00	4,15	2,26	4,82
2	0,98%	9,94	4,41	9,94	4,66	3,14	4,41	3,75	4,79
3	6,66%	17,67	4,21	17,67	4,49	7,93	4,21	8,82	4,68
4	7,22%	20,67	4,36	20,67	4,43	9,93	4,36	12,92	4,60

TABLE 4

Storage capacity for samples with moisture 70%. G values in m³/t

ϕ 4,8									
50°C					80°C				
Sample	TOC	G_a	G_f	G_{aAmbr}	G_{fAmbr}	G_a	G_f	G_{aAmbr}	G_{fAmbr}
1	0,3%	6,98	1,11	6,98	0,99	2,00	1,11	2,26	1,09
2	0,98%	9,94	1,09	9,94	0,92	3,14	1,09	3,75	1,06
3	6,66%	17,67	1,33	17,67	0,76	7,93	1,33	8,82	0,95
4	7,22%	20,67	0,99	20,67	0,69	9,93	0,99	12,92	0,86
ϕ 9,5									
50°C					80°C				
Sample	TOC	G_a	G_f	G_{aAmbr}	G_{fAmbr}	G_a	G_f	G_{aAmbr}	G_{fAmbr}
1	0,3%	6,98	1,92	6,98	2,10	2,00	1,92	2,26	2,20
2	0,98%	9,94	2,04	9,94	2,04	3,14	2,04	3,75	2,17
3	6,66%	17,67	1,94	17,67	1,87	7,93	1,94	8,82	2,06
4	7,22%	20,67	2,01	20,67	1,81	9,93	2,01	12,92	1,97

Figure 9 shows results for shale storage capacity for 4.8% porosity shale, 35% water saturation and 80°C reservoir temperature. Samples with lower TOC have amount of storage gas approx. 5 to 8 m³/t, while samples with higher TOC have amount of gas storage approx. 10 to 15 m³/t.

Figure 10 shows results for shale storage capacity for 9.5% porosity shale, 35% water saturation and 50°C reservoir temperature. Samples with lower TOC have amount of storage gas approx. 9 to 15 m³/t, while samples with higher TOC have amount of gas storage approx. 20 to 25 m³/t.

Figure 11 shows results for shale storage capacity for 9.5% porosity shale, 35% water saturation and 80°C reservoir temperature. Samples with lower TOC have amount of storage gas approx. 4 to 9 m³/t, while samples with higher TOC have amount of gas storage approx. 11 to 18 m³/t.

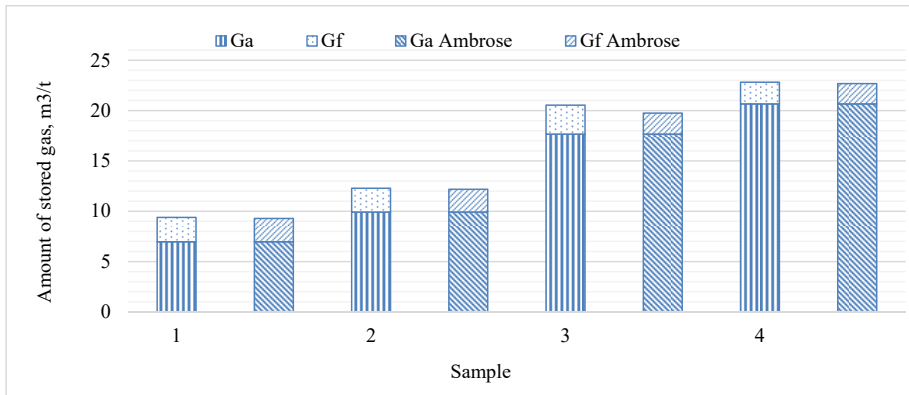


Fig. 8. Shale storage capacity for 4.8% porosity shale, 35% water saturation and 50°C reservoir temperature – standard method compared to the modified Ambrosio method

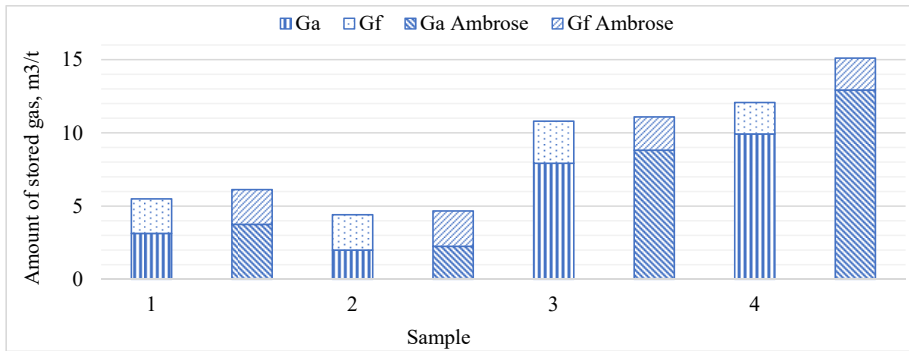


Fig. 9. Shale storage capacity for 4.8% porosity shale, 35% water saturation and 80°C reservoir temperature – standard method compared to the modified Ambrosio method

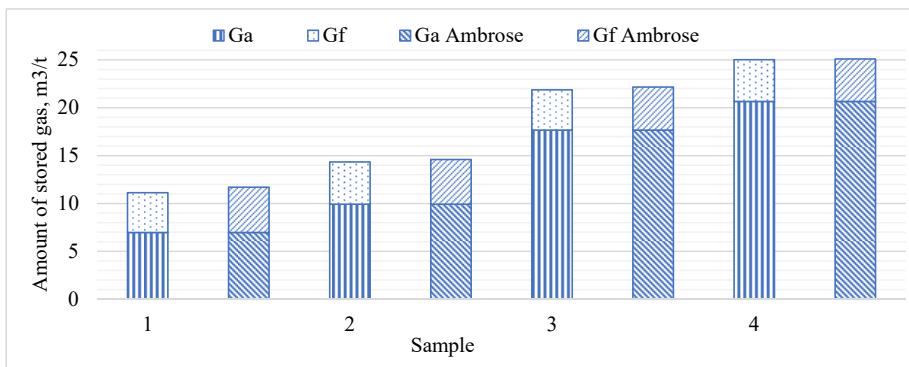


Fig. 10. Shale storage capacity for 9.5% porosity shale, 35% water saturation and 50°C reservoir temperature – standard method compared to the modified Ambrosio method

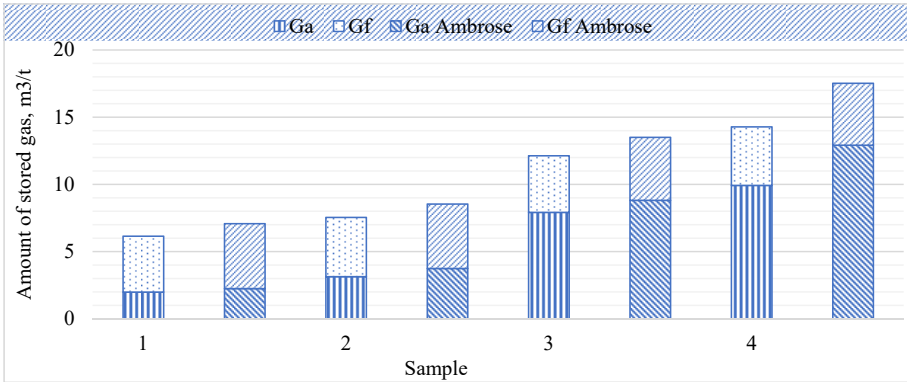


Fig. 11. Shale storage capacity for 9.5% porosity shale, 35% water saturation and 80°C reservoir temperature – standard method compared to the modified Ambrosio method

Figure 12 shows results for shale storage capacity for 4.8% porosity shale, 70% water saturation and 50°C reservoir temperature. Samples with lower TOC have amount of storage gas approx. 8 to 12 m³/t, while samples with higher TOC have amount of gas storage approx. 19 to 22 m³/t.

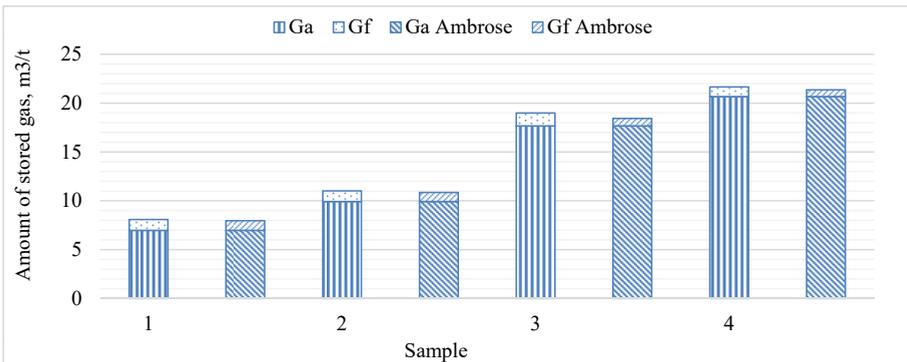


Fig. 12. Shale storage capacity for 4.8% porosity shale, 70% water saturation and 50°C reservoir temperature – standard method compared to the modified Ambrosio method

Figure 13 shows results for shale storage capacity for 4.8% porosity shale, 70% water saturation and 80°C reservoir temperature. Samples with lower TOC have amount of storage gas approx. 3 to 5 m³/t, while samples with higher TOC have amount of gas storage approx. 9 to 14 m³/t.

Figure 14 shows results for shale storage capacity for 9.5% porosity shale, 70% water saturation and 50°C reservoir temperature. Samples with lower TOC have amount of storage gas approx. 8 to 13 m³/t, while samples with higher TOC have amount of gas storage approx. 19 to 23 m³/t.

Figure 15 shows results for shale storage capacity for 9.5% porosity shale, 70% water saturation and 80°C reservoir temperature. Samples with lower TOC have amount of storage gas approx. 3 to 6 m³/t, while samples with higher TOC have amount of gas storage approx. 9 to 15 m³/t.

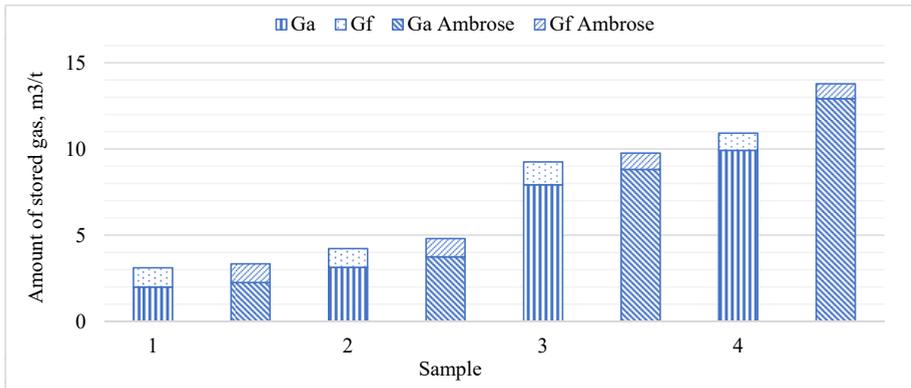


Fig. 13. Shale storage capacity for 4.8% porosity shale, 70% water saturation and 80°C reservoir temperature – standard method compared to the modified Ambrosio method

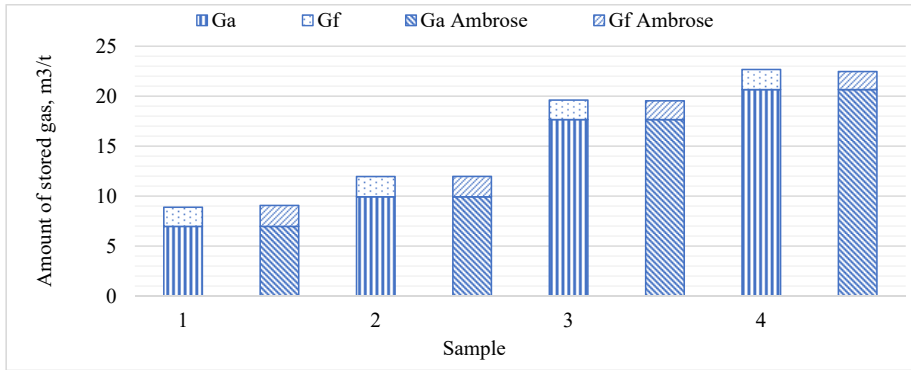


Fig. 14. Shale storage capacity for 9.5% porosity shale, 70% water saturation and 50°C reservoir temperature – standard method compared to the modified Ambrosio method

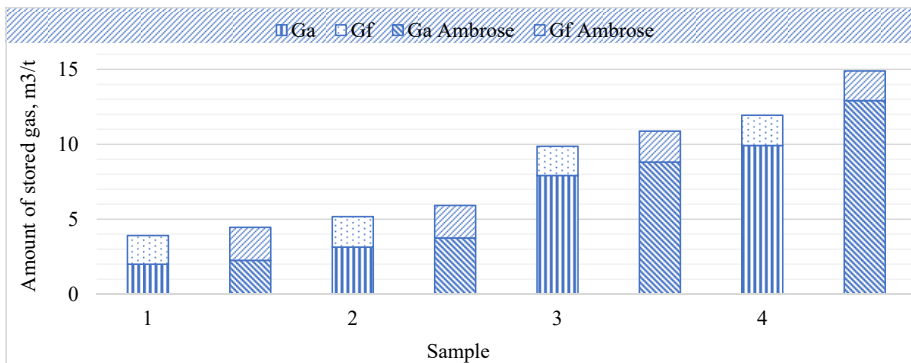


Fig. 15. Shale storage capacity for 9.5% porosity shale, 70% water saturation and 80°C reservoir temperature – standard method compared to the modified Ambrosio method

4. Conclusions

Several factors influencing the sorption capacity have been identified: total organic content, porosity, temperature and moisture. Clay minerals also have an impact on the sorption capacity as the sample 2 with lowest TOC has the highest total clay mineral content where sorption capacity slightly exceeds that of Sample 1 with higher TOC and lower clay content. This phenomena has been developed further and is the scope of a separate study under publication. There is a positive relationship between the total content of organic matter and the stored volume, and the porosity of the material and the stored volume. Temperature and amount of stored gas is inversely proportional, which is a result of earlier mentioned link between sorption capacity and temperature. Storage capacity is lower with increasing water saturation.

The total organic content is a place of formation of many active centers where gas is willingly sorbed therefore its content increases the capacity of gas which can be stored in shale. Porosity affects sorption capacity in at least two ways: increase volume where free gas can gather and surface available for adsorbing gas, although its influence does not seem as strong as TOC. The sorption capacity decreases with the moisture of the sample – water makes it difficult for the gas to contact the surface on which it can sorb and reducing the chance of gas to transit from free to bound state. The temperature lowers the sorption capacity by half.

Although all factors are influencing the potential CO₂ storage capacity in shales, the greatest influence has total organic content, as with constant deposit conditions, the TOC is modifying sorption capacity the most.

When examining if shale formation is suitable for gas storage a several aspects should be taken under consideration. One of them is estimating the volume of gas that can be stored in shale deposits. The attention should be paid first of all on total organic content – the higher its share in shale composition, the larger volume can be stored in rock. Moisture is naturally tied with shales, reservoirs chosen for storage should be as dry as it is possible. Temperature in depths suitable for storing is rather constant and oscillating around 80°C and porosity has less influence than other factors which means should be considered as the least important factor. The content of clay minerals should also be taken into consideration as it might increase the sorption capacity particularly in shales with low TOC content.

References

- [1] A. Szurlej, P. Janusz, Natural gas economy in the United States and European markets. *Gospodarka Surowcami Mineralnymi (Mineral Resources Management)* **29** (4), 77-94 (2013). DOI: <https://doi.org/10.2478/gospo-2013-0043>
- [2] B. Dudley, BP Statistical Review of World Energy **4** (2019).
- [3] J. Siemek, M. Kaliski, S. Rychlicki, P. Janusz, S. Sikora, A. Szurlej, Wpływ shale gas na rynek gazu ziemnego w Polsce. *Rynek Energii* **5**, 118-124 (2011).
- [4] K. Król, A. Dynowski, Eksploatacja gazu ziemnego z formacji łupkowych w Polsce – nadzieje i fakty (komunikat). *Bezp. Pr. Ochr. Śr. w Gór.* **10** (2015).
- [5] M. Iijima, T. Nagayasu, T. Kamijyo, S. Nakatani, MHI's Energy Efficient Flue Gas CO₂ Capture Technology and Large Scale CCS Demonstration Test at Coal-fired Power Plants in USA. *Mitsubishi Heavy Industries Technical Review* **49** (1), 37-43 (2012).
- [6] R. Khosrokhavar, Mechanisms for CO₂ sequestration in geological formations and enhanced gas recovery. Springer Theses (2016). DOI: <https://doi.org/10.4233/uuid:a27f5c1d-5fd2-4b1e-b757-8839c0c4726c>

- [7] D. Liu, Y. Li, S. Yang, R.K. Agarwal, CO₂ sequestration with enhanced shale gas recovery. *Energy Sources, Part A: Recovery, Utilization, and Environmental Effects* **43** (24) 1-11 (2019). DOI: <https://doi.org/10.1080/15567036.2019.1587069>
- [8] R. Heller, M. Zoback, Adsorption of methane and carbon dioxide on gas shale and pure mineral samples. *Journal of Unconventional Oil and Gas Resources* **8**, 14-24 (2014). DOI: <https://doi.org/10.1016/j.juogr.2014.06.001>
- [9] J.A. Cecilia, C. García-Sancho, E. Vilarrasa-García, J. Jiménez-Jiménez, E. Rodríguez-Castellón, Synthesis, Characterization, Uses and Applications of Porous Clays Heterostructures: A Review. *Chem. Rec.* **18**, 1085-1104 (2018). DOI: <https://doi.org/10.1002/tcr.201700107>
- [10] O.P. Ortiz Cancino, D. Peredo Mancilla, M. Pozo, E. Pérez, D. Bessieres, Effect of Organic Matter and Thermal Maturity on Methane Adsorption Capacity on Shales from the Middle Magdalena Valley Basin in Colombia. *Energy Fuels* **31**, 11698-11709 (2017). DOI: <https://doi.org/10.1021/acs.energyfuels.7b01849>
- [11] S. Zhou, H. Xue, Y. Ning, W. Guo, Q. Zhang, Experimental study of supercritical methane adsorption in Longmaxi shale: Insights into the density of adsorbed methane. *Fuel* **211**, 140-148 (2018). DOI: <https://doi.org/10.1016/j.fuel.2017.09.065>
- [12] H. Bi, Z. Jiang, J. Li, P. Li, L. Chen, Q. Pan, Y. Wu, The Ono-Kondo model and an experimental study on supercritical adsorption of shale gas: A case study on Longmaxi shale in southeastern Chongqing, China. *J. Nat. Gas Sci. Eng.* **35**, 114-121 (2016). DOI: <https://doi.org/10.1016/j.jngse.2016.08.047>
- [13] M. Gasparik, P. Bertier, Y. Gensterblum, A. Ghanizadeh, B.M. Krooss, R. Littke, Geological controls on the methane storage capacity in organic-rich shales. *Int. J. Coal Geol.*, Special issue: Adsorption and fluid transport phenomena in gas shales and their effects on production and storage **123**, 34-51 (2014). DOI: <https://doi.org/10.1016/j.coal.2013.06.010>
- [14] X. Luo, S. Wang, Z. Wang, Z. Jing, M. Lv, Z. Zhai, T. Han, Adsorption of methane, carbon dioxide and their binary mixtures on Jurassic shale from the Qaidam Basin in China. *Int. J. Coal Geol.* **150**, 210-223 (2015). DOI: <https://doi.org/10.1016/j.coal.2015.09.004>
- [15] L. Wang, Q. Yu, The effect of moisture on the methane adsorption capacity of shales: A study case in the eastern Qaidam Basin in China. *J. Hydrol.* **542**, 487-505 (2016). DOI: <https://doi.org/10.1016/j.jhydrol.2016.09.018>
- [16] S.M. Kang, E. Fathi, R.J. Ambrose, I.Y. Akkutlu, R.F. Sigal, Carbon Dioxide Storage Capacity of Organic-Rich Shales. *SPE J.* **16**, 842-855 (2011). DOI: <https://doi.org/10.2118/134583-PA>
- [17] D.L. Gautier, J.K. Pitman, R.R. Charpentier, T. Cook, T.R. Klett, C.J. Schenk, Potential for Technically Recoverable Unconventional Gas and Oil Resources in the Polish-Ukrainian Foredeep. *USGS Fact Sheet*, 2012-3102 (2012).
- [18] R. McCarthy, V. Arp, A New Wide Range Equation of State for Helium. *Advances in Cryogenic Engineering* **35**, 1465-1475 (1990).
- [19] R. Span, W. Wagner, A New Equation of State for Carbon Dioxide Covering the Fluid Region from the Triple-Point Temperature to 1100 K at Pressures up to 800 MPa. *Journal of Physical and Chemical Reference Data* **25** (6), 1509-1596 (1996). DOI: <https://doi.org/10.1063/1.555991>
- [20] U. Setzmann, W. Wagner, A New Equation of State and Tables of Thermodynamic Properties for Methane Covering the Range from the Melting Line to 625 K at Pressures up to 100 MPa. *Journal of Physical and Chemical Reference Data* **20**, 1061-1155 (1991). DOI: <https://doi.org/10.1063/1.555898>
- [21] M. Lutynski, M. A. Gonzalez Gonzalez, Characteristics of carbon dioxide sorption in coal and gas shale – The effect of particle size. *Journal of Natural Gas Science and Engineering* **28**, 558-565. DOI: <https://doi.org/10.1016/j.jngse.2015.12.037>
- [22] R. Aguilera, Shale gas reservoirs: Theoretical, practical and research issues. *Petroleum Research* **1** (1), 10-26 (2016). DOI: [https://doi.org/10.1016/S2096-2495\(17\)30027-3](https://doi.org/10.1016/S2096-2495(17)30027-3)
- [23] H. Belyadi, E. Fathi, F. Belyadi, Hydraulic fracturing in unconventional reservoirs: theories, operations, and economic analysis. *Gulf Professional Publishing* (2016).
- [24] K. Sepehrnoori, Y. Wei, *Shale Gas and Tight Oil Reservoir Simulation*. Elsevier (2018). DOI: <https://doi.org/10.1016/C2017-0-00263-X>
- [25] R.J. Ambrose, R.C. Hartman, M. Diaz-Campos, I.Y. Akkutlu, C.H. Sondergeld, New Pore-scale Considerations for Shale Gas in Place Calculations. Presented at the SPE Unconventional Gas Conference, Society of Petroleum Engineers (2010). DOI: <https://doi.org/10.2118/131772-MS>
- [26] R.J. Ambrose, R.C. Hartman, M. Diaz Campos, I.Y. Akkutlu, C.H. Sondergeld, Shale Gas-in-Place Calculations Part I: New Pore-Scale Considerations. *Spe Journal* **17** (01), 219-229 (2012). DOI: <https://doi.org/10.2118/131772-PA>
- [27] P. Such, Co to właściwie znaczy porowatość skał łupkowych. *Nafta-Gaz LXX* (7), 411-415 (2014).